JOURNAL OF MATERIALS SCIENCE 30 (1995) 5078–5086

Interpretation of the impedance spectroscopy of cement paste via computer modelling

Part III *Microstructural analysis of frozen cement paste*

R. A. OLSON, B. J. CHRISTENSEN, R. T. COVERDALE, S. J. FORD, G. M. MOSS, H. M. JENNINGS, T. O. MASON
Center for Advanced Cement-Based Materials, Northwestern University, Evanston, IL 60208, USA

E. J. GARBOCZI
National Institute of Standards and Technology, 226/B350, Building Materials Division, Gaithersburg, MD 20899, USA

The d.c. conductivity, σ, and low-frequency relative dielectric constant, k, of Portland cement paste were monitored, using impedance spectroscopy, during cooling from room temperature down to −50 °C. Dramatic decreases in the values of σ and k, as great as two orders of magnitude, occurred at the initial freezing point of the aqueous phase in the macropores and larger capillary pores. This result provides strong experimental support for the dielectric amplification mechanism, proposed in Part II of this series, to explain the high measured low-frequency relative dielectric constant of hydrating Portland cement paste. Only gradual changes in the electrical properties were observed below this sudden drop, as the temperature continued to decrease. The values of σ and k of frozen cement paste, at a constant temperature of −40 °C, were dominated by properties of calcium–silicate–hydrate (C–S–H) and so increased with the degree of hydration of the paste, indicating a C–S–H gel percolation threshold at a volume fraction of approximately 15%–20%, in good agreement with previous predictions. Good agreement was found between experimental results and digital-image-based model computations of σ at −40 °C. Freeze–thaw cycling caused a drop in the dielectric constant of paste in the unfrozen state, indicating that measurements of k could be useful for monitoring microstructural changes during freeze-thaw cycling and other processes that gradually damage parts of the cement paste microstructure.

1. Introduction

Impedance spectroscopy (IS) is an electrical technique that has been used to characterize the microstructure of cement paste, providing useful information about the relationships between microstructure, electrical properties, and chemical processes during the hydration of cement paste [1–9]. The IS experiment consists of applying an alternating current, of small enough amplitude to be in the linear response regime, to a cement paste sample and measuring the impedance as a function of frequency. The measurement of impedance can be made rapidly and easily while the sample is hydrating, without altering its microstructure or drying the sample.

Parts I [10] and II [11] of this series studied the relationships between the d.c. conductivity, σ [10], and low-frequency relative dielectric constant, k [11], and the microstructure of cement paste, using IS measurements interpreted by digital-image-based computer models. One main experimental finding was that the value of k for cement paste can be very high [11]. The value of k increases sharply during the first 10–15 h hydration to a value as high as 10^4–10^5, then decreases gradually to a value near 10^3, as shown by Fig. 1 [2, 4, 11]. The high values are surprising, because none of the components of the cement paste have such high values. The aqueous phase (dissolved inorganic ions in water), which is the single pure phase with the highest value of k, has $k \approx 80$. Calcium silicate hydrate (C–S–H) gel contains small water-filled pores, and although its overall dielectric constant is relatively high, perhaps about $k = 10^3$ [2, 4], it cannot account for cement paste values on the order of $k = 10^5$, especially at early stages of hydration where not much C–S–H is present.

In Part II of this series, a "dielectric amplification" mechanism was proposed [11] based on a geometric amplification within the microstructure on

0022–2461

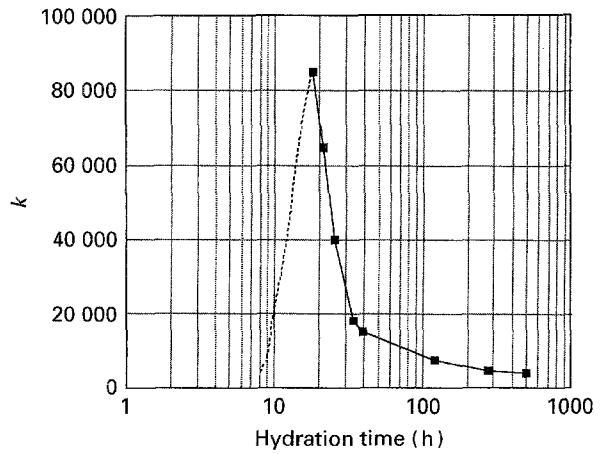

Figure 1 Relative dielectric constant versus hydration time for a Portland cement paste of w/c ratio 0.4. (- - -) A slight uncertainty in the early measurements due to the high frequency required to obtain the data (taken from [2, 4, 11]).

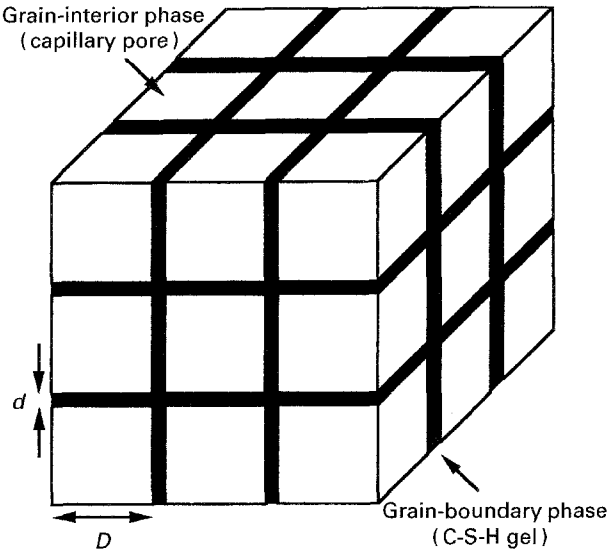

Figure 2 Schematic diagram of the brick layer model of a grain-boundary ceramic and its relationship to cement paste [12].

a micrometre scale. The proposed mechanism is a microstructure of interlocking C–S–H gel and pore water with a structure in some ways similar to that of a grain-boundary ceramic [12], where the interconnecting layers of C–S–H act as low σ, high k grain boundaries, and the capillary pores act as high σ, low k grains, as shown schematically in three dimensions in Fig. 2. Because the current is carried mainly by the pore fluid ($\sigma_0 = 4$–$6\ \mathrm{S\,m^{-1}}$ for typical Portland cement pastes), a large capacitance could result from thin layers of C–S–H gel within the capillary pore network. Porous rocks saturated with an electrolytic solution, having microstructures in some respects similar to that of hardened cement paste, also display high dielectric constants [13]. Similarly, porous alumina saturated with brine solution has a low-frequency relative dielectric constant on the order of 10^6 [14].

This amplification mechanism can be demonstrated in the following simple example. A composite parallel plate capacitor, shown in Fig. 3a, has a capacitance

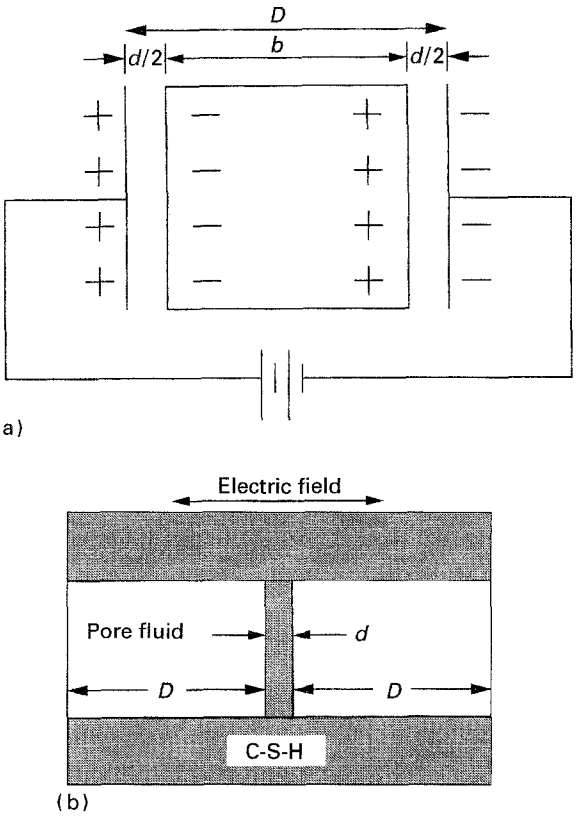

Figure 3 (a) A schematic diagram of a parallel plate capacitor, where D is the distance between the plates, b the thickness of the dielectric substance, and d the space between the dielectric substance and the plates [3]. (b) A schematic diagram of the arrangement of C–S–H and capillary pores in cement paste, in analogy to (a) (taken from [11]).

that is controlled by its D/d ratio, as given by

$$\begin{aligned} C &= k\varepsilon_0 (A/D) \\ &= k_s\varepsilon_0 [A/(D-b)] \\ &= k_s\varepsilon_0 (A/d) \\ &= k_s\varepsilon_0 (D/d)\,(A/D) \end{aligned} \quad (1)$$

where C is the capacitance, D the distance between the plates, b the thickness of the conducting material between the plates, k_s the relative dielectric constant of the substance in the $d/2$ width gaps, ε_0 the permittivity of free space, k the effective dielectric constant of the entire composite parallel plate capacitor, and A is the cross-sectional area of the electrodes [2]. The resulting overall relative dielectric constant

$$k = k_s (D/d) \quad (2)$$

can be very large, depending on the D/d ratio. This is the type of amplification observed in grain-boundary ceramics, where D is the grain size of the conductive grains and d the thickness of the more insulating grain boundaries.

The dielectric constant of each "C–S–H capacitor" in the microstructure of cement paste is also controlled by its D/d ratio, as shown by the schematic diagram in Fig. 3b, where d is the thickness of the C–S–H layer and D is the size of the capillary pore. Initially, as C–S–H is produced and projects into the capillary network, the dielectric constant of the paste

increases. At some point, however, the D/d ratio of each capillary pore: C–S–H "capacitor" begins to decrease. This is due both to the increase of the value of d, via hydration growth of C–S–H, and the corresponding reduction in the value of D, as pore water is consumed and porosity and pore size decreases. Reducing the value of D/d causes the dielectric constant of the entire sample to also decrease. Part II showed that, unlike grain-boundary ceramics, the high conductivity phase, which in cement paste is the capillary pore space, did not need to be disconnected in order to generate a high dielectric constant. It was also suggested that this same mechanism, acting at the nanometre scale in the nanometre-size C–S–H pores, was responsible for the relatively high value of $k \approx 10^3$ for C–S–H.

The electrical coupling between the pore fluid in the capillary pores and the high values of k assumed to be taking place in the proposed dielectric amplification mechanism implies a method of independently checking the validity of this mechanism. Because the freezing point of pore fluid depends on the size of the pore it occupies [15], a phenomenon associated with freezing-point depression in small pores, changes in electrical properties with decreasing temperature can be attributed to specific size classes of pores. In the present study, the pore solution in the capillary pores was frozen in order to change the main conducting path from the capillary porosity to the C–S–H gel. The smaller pores in the C–S–H phase freeze at lower temperatures than the larger capillary pores, so that the conductivity of the C–S–H phase, while still lower than its value at room temperature, becomes significantly higher than the conductivity of the capillary pores filled with frozen pore fluid. "Turning off" the high conductivity of the capillary pores should then have a substantial effect on the value of k, if the proposed dielectric amplification mechanism is valid.

2. Experimental procedure

Cement paste was prepared by adding deionized water to ordinary Portland cement and mixing with a spatula for 1 min. Samples of dimensions 30 mm × 15 mm × 2.5 mm were cast into plastic moulds. Stainless steel electrodes of dimensions 7.5 mm × 7.5 mm were placed into the wet cement paste approximately 20 mm apart. All samples were stored in an airtight chamber above a pool of lime-saturated water to prevent drying.

The freezing apparatus, shown schematically in Fig. 4, consisted of an insulated thermoelectric stainless steel plate controlled by a variable power source. The cold chamber consisted of a stainless steel cylinder open at both ends and a stainless steel lid. A thermistor (10 kΩ ± 1% at 25 °C) connected to a multimeter was used to monitor the temperature inside the chamber. Two 160 mm long 24 gauge wires were run through the top of the cold chamber and attached to the electrodes in the sample. The opposite ends were connected to the impedance analyser via a two-electrode connecting jack.

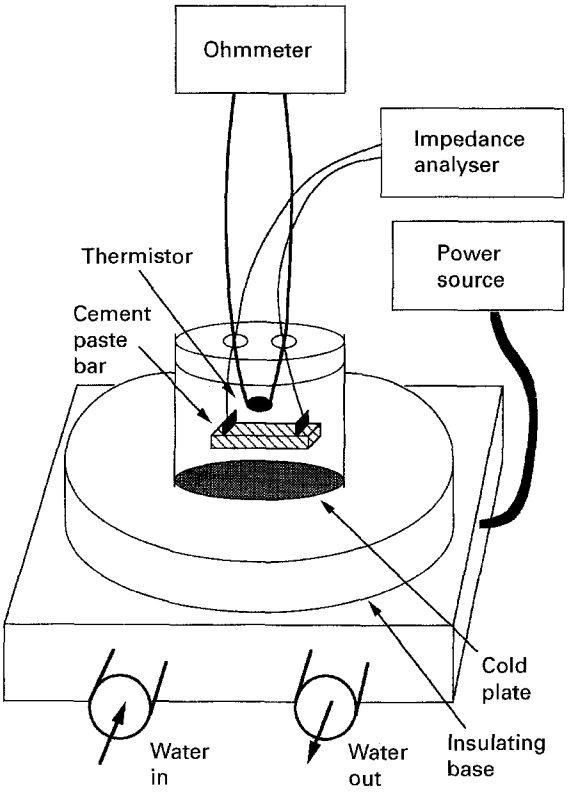

Figure 4 A schematic diagram of the freezing/IS apparatus used to obtain the experimental results reported in this paper.

Two impedance analysers, a Hewlett–Packard Model 4192A and a Schlumberger Model 1260*, with frequency ranges of 13 MHz to 5 Hz and 32 MHz to 10 μHz, respectively, were used. Impedance data were collected within a frequency range of 10 MHz to 10 Hz using a personal computer interfaced to the impedance analyser, and were analysed using "Equivalent Circuit" [16]. The resistance and capacitance of each sample were determined by fitting the experimental impedance curves. Variations in the fitting procedure resulted in only about a 20% difference in the calculated dielectric constant. This amount of precision was considered to be acceptable for this experiment. Data for frequencies above 3 MHz were not used because of the known unreliability of impedance data in this frequency range [4].

High-frequency measurements were corrected to account for the residual inductive and capacitive effects of the wires and the internal resistance of the impedance analyser. Because these corrections for the frozen pastes resulted in a change of less than 1% for the resistance, and less than 5% for the capacitance, the corrections were not actually required to achieve an acceptable level of accuracy. More details of the measurement process can be found elsewhere [2, 4, 10, 11].

3. Freezing of water in cement paste pores

The formation of ice within a pore is dependent on the size of the pore. Nucleation of ice crystals becomes

*Certain commercial companies are named in order to specify adequately the experimental procedure. This in no way implies endorsement or recommendation by the national institute of Standards and Technology.

more difficult as pore size decreases. The freezing point depression of pore water is related to the pore radius by the well-known Gibbs–Thomson equation [17]

$$\ln(T/T_0) = -2\Delta GV/\Delta Hr \quad (3)$$

where T is the temperature of the water in the pore (K), T_0 is the freezing point, $\Delta G = G$(matrix/ice) $- G$(matrix/water), G is the interfacial energy, V the molar volume of water, ΔH the latent heat of fusion, and r the pore radius [18]. As the pore radius decreases, the freezing point of water in the pore decreases. This effect has been observed in many porous materials for many different fluids [15], and is also observed for water in cement paste. Calorimetric results of hardened cement paste [18–22] from 10 °C to − 60 °C show three well-defined peaks at approximately − 8, − 23, and − 40 °C. Ice formation does not occur above − 8 °C due to the freezing point depression of the pore water, caused by both pore-size effects, as given by Equation 3, and the high ionic strength of the pore solution. The peak at − 8 °C is due to freezing bulk water in the macropores. The peak at − 23 °C corresponds to the freezing of the smaller capillary pores, while the rather broad peak at − 40 °C represents the low-temperature transition of supersaturated solution in gel pores. Very little additional freezing occurs below this last peak. Calorimetric studies have been performed down to a temperature of − 175 °C, and there is no indication of bulk ice formation below this point [18, 19]. There is, however, some evidence for a freezing of an adsorbed water film at approximately − 90 °C [20, 21].

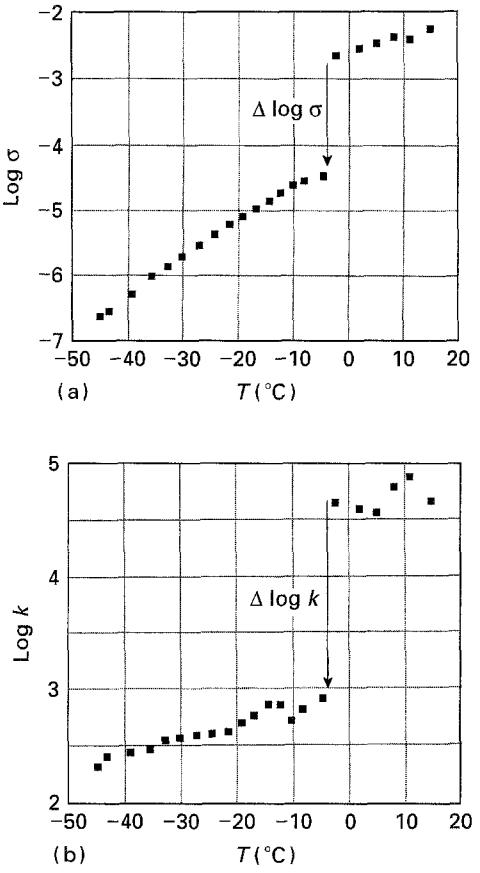

Figure 5 (a) Log d.c. conductivity versus temperature for a 0.4 w/c ratio cement paste hydrated 15 h. The quantity $\Delta \log \sigma$ is defined in the graph by the vertical arrow, indicating the magnitude of the abrupt drop in the conductivity near − 8 °C. (b) Log relative dielectric constant versus temperature for a 0.4 w/c ratio cement paste hydrated 15 h.

4. Dielectric amplification mechanism: results and discussion

The conductivity, σ, and the relative dielectric constant k of each sample were measured from room temperature down to − 50 °C. Typical plots of σ and k as a function of temperature for a cement paste of 0.4 w/c ratio (w/c = weight ratio of water to cement used in making the cement paste), hydrated for 15 h prior to freezing, are displayed in Fig. 5a and b, respectively.

4.1. Effect of freezing on the d.c. conductivity

As shown by Fig. 5a, log σ decreases linearly with temperature down to about − 5 °C, drops sharply about two orders of magnitude, then decreases linearly again. Some samples were cooled to temperatures below − 100 °C to determine if any other sharp drops in the conductivity existed, but the log σ value was linear throughout this region. This is displayed in Fig. 6, which represents a paste of 0.4 w/c ratio, as in Fig. 5a, but for a slightly longer hydration time of 18 h. The large conductivity drop ($\Delta \log \sigma$, defined in Fig. 5a) occurs within the same temperature range as the freezing point of the large capillary pores, as determined by differential scanning calorimetry (DSC) [18–24], so it is reasonable to conclude that the drop

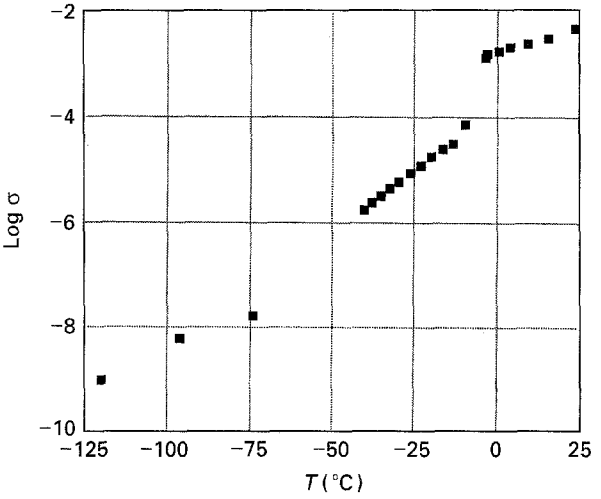

Figure 6 Log d.c. conductivity versus temperature for a 0.4 w/c ratio cement paste hydrated 18 h, and taken to lower temperatures.

is a result of the freezing of bulk and capillary water. When this water freezes, the mobility of the ions that carry the electrical current (mainly Na^+, K^+, and OH^- [1]) is sharply reduced, and thus the conductivity of this phase is sharply reduced as well. As the smaller gel pores freeze at lower temperatures, the conductivity continues to decrease continuously. This

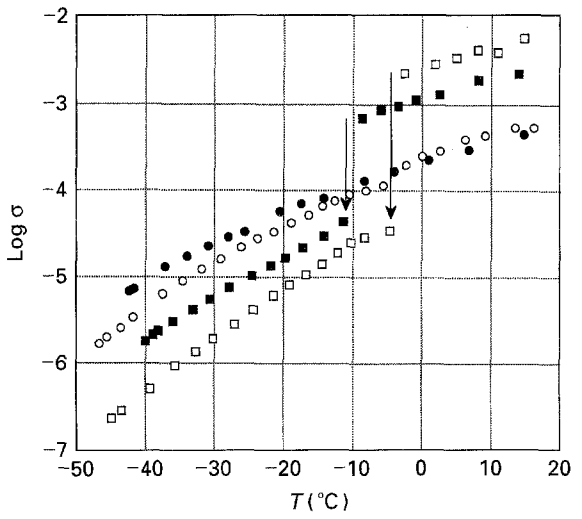

Figure 7 Log d.c. conductivity versus temperature for a 0.4 w/c ratio cement paste hydrated (□) 15, (■) 26, (○) 200 h and (●) 40 days.

large drop at about − 8 °C is probably due to the freezing of larger capillary pores that are percolated or connected at short hydration times. This point is made clearer in Fig. 7.

As hydration continues and the capillary water is consumed, more C–S–H is produced, and Δ log σ decreases at a given temperature. Fig. 7 is a plot of the log σ versus temperature for four pastes of w/c ratio 0.4 with hydration times of 15, 26, 200 h and 40 days. Note how Δ log σ decreases with increasing time, until, at about 40 days, there is essentially no abrupt large drop in the log σ versus T curve. After 40 days hydration, a 0.4 w/c ratio cement paste has very little capillary porosity remaining, and this porosity is almost certainly discontinuous. When the larger capillary pores are well-percolated and have a relatively large volume fraction, they will dominate the overall value of the conductivity. Switching off their conductivity by freezing causes a steep drop in the conductivity of the paste. As more and more of the capillary pores become discontinuous with the hydration of the paste, less and less of a steep drop in conductivity is seen upon freezing, because the overall conductivity is no longer dominated by the percolated capillary pores. After the percolation threshold for the capillary pores is reached, there is still a decrease in conductivity upon freezing, but no steep "discontinuous" drop, as the capillary pores, being disconnected, no longer control the conductivity of the cement paste.

The percolation threshold for the larger capillary pores has been predicted to be 18%, independent of w/c ratio [25]. For a paste of w/c ratio 0.4, the critical degree of hydration needed to achieve this porosity is approximately 0.65, where the degree of hydration is the volume fraction of cement that has reacted. This would correspond to a hydration time somewhere between 8 and 40 days, so the above predicted behaviour for Δ log σ is in agreement with the data shown in Fig. 7.

4.2. Effect of freezing on the dielectric constant of cement paste

The behaviour of the dielectric constant as a function of decreasing temperature is very similar to the behaviour of the conductivity, as shown by Fig. 5b. The value of log k is relatively constant with change in temperature down to about − 5 °C, where it drops sharply by two orders of magnitude. Beyond this point, log k is again relatively constant with change in temperature. Log k of samples cooled below − 100 °C remained relatively unchanged in the temperature region below the drop, as shown by Fig. 8.

When tap water is frozen, k drops from a value of about 80 at room temperature, to a value of about 5 at temperatures below 0 °C. In previous studies, the dielectric constant of extracted pore solution at room temperature was found to be similar to that of water [2, 4]. However, the dielectric constant of frozen pore solution is difficult to determine because the solution does not freeze completely at a specific temperature. Multiple arcs appear in the impedance spectra at low temperatures, which suggests that multiple phases precipitate during freezing. For example, a pore solution extracted from a cement paste hydrated for 15 h and then tested at − 50 °C displays four separate arcs, as shown in Fig. 9. The phase separation, with its

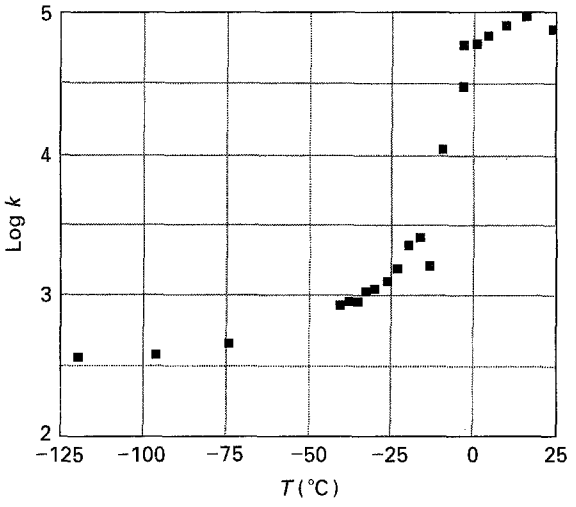

Figure 8 Log relative dielectric constant versus temperature for a 0.4 w/c ratio cement paste hydrated 18 h, and taken to lower temperatures.

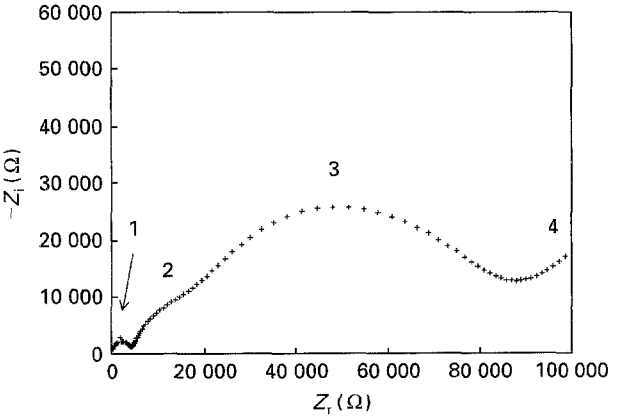

Figure 9 Impedance response of frozen pore solution at − 50 °C. The numbers indicate the four (at least) arcs which make up the impedance response.

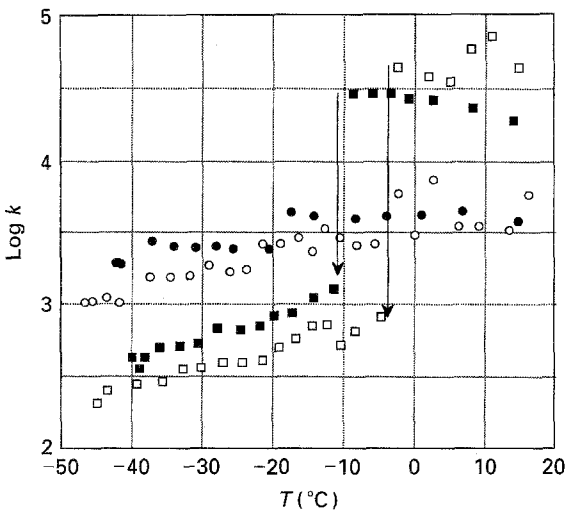

Figure 10 Log relative dielectric constant versus temperature for a 0.4 w/c ratio cement paste hydrated (□) 15, (■) 26, (○) 200 h and (●) 40 days.

resulting multiple arc response, makes it impossible to estimate the dielectric constant accurately. Because of the small size of pores, phase separation may not occur during freezing of cement paste. According to Yoon *et al.* [26], freshly mixed cement paste with a w/c ratio of 0.4 has a dielectric constant of about 24 at $-30\,^{\circ}C$, so it is safe to assume that the dielectric constant of frozen pore solution is of the same order as the dielectric constant of frozen tap water.

Although the dielectric constant of pore solution decreases when it freezes, this cannot be the only cause for the drop in the dielectric constant of cement paste. The drop in k for the pore solution is at most about one order of magnitude, compared to the largest drop in k for cement paste being up to three orders of magnitude* [27] measured for an 0.7 w/c ratio cement paste. This result is strong evidence for the dielectric amplification mechanism proposed in Part II [11] of this series. This dielectric amplification mechanism is clearly almost eliminated when the capillary pores freeze and lose their high conductivity. When this happens the microstructure changes from one in which the layers of C–S–H gel act as capacitors within the conductive capillary porosity to one in which the interconnected C–S–H gel becomes the most conductive pathway, embedded in the much less conductive capillary pores. The relative value of the conductivity of frozen pore solution and C–S–H are discussed in Section 5 below.

Fig. 10 is a plot of log k versus temperature for four pastes of w/c ratio 0.4 with hydration times of 15, 26, 200 h and 40 days. Notice how $\Delta \log k$ decreases with time until at about 40 days there is only a minimal drop. The behaviour of $\Delta \log k'$ essentially tracks that of $\Delta \log \sigma$. After the capillary pores become disconnected, the dielectric amplification mechanism loses its effectiveness. Turning off the conductivity of the capillary pores by freezing then has relatively little effect on the value of k.

5. Electrical properties of frozen cement paste at $-40\,^{\circ}C$

The conductivity and the dielectric constant of frozen cement paste, at temperatures lower than $-8\,^{\circ}C$, increased with hydration time, as shown in Figs 7 and 10. Assuming that in the frozen paste the C–S–H gel has the highest conductivity and the highest dielectric constant, these electrical properties of the paste would be expected to increase with time, as the degree of hydration and therefore the amount of C–S–H has increased.

To enable quantitative comparison between experimental and computational results for the d.c. conductivity, the normalized conductivity was used. This is defined as σ/σ_{CSH}, where σ_{CSH} is the conductivity of the pure C–S–H phase at $-40\,^{\circ}C$, as determined below. The quantity σ is the measured electrical property at $-40\,^{\circ}C$ of the frozen pastes. The temperature of $-40\,^{\circ}C$ was chosen because it is the point at which most of the capillary porosity is frozen, but most of the gel porosity is still unfrozen. This leaves the C–S–H gel as the only conducting phase, and the frozen capillary porosity as an insulating phase. No significant changes in σ or k were observed between -5 and $-40\,^{\circ}C$, because the remaining unfrozen capillary porosity is disconnected after the larger capillary pores freeze.

The volume fraction of C–S–H gel, ϕ_{CSH}, which is then expected to be the primary variable, was calculated as follows

$$\phi_{CSH} = 0.53\alpha/(w_0/c + 0.315) \quad (4)$$

where w_0/c is the initial water to cement ratio, and α the degree of hydration [28]. The degree of hydration was approximated using data in [4].

As shown by Fig. 11, the experimental normalized conductivity increases with the volume fraction of C–S–H gel for frozen pastes of w/c ratios 0.4 and 0.7. If C–S–H gel is indeed the most conductive phase in the matrix, the conductivity of the paste would be expected to increase as hydration proceeds and more C–S–H gel is produced, as observed. Note, too, how the conductivity of the frozen paste is independent of w/c ratio, also indicating that the conductivity depends on the C–S–H content only.

Interestingly, the normalized conductivity of frozen paste does not begin to increase significantly until the C–S–H gel reaches a volume fraction of about 0.20. The percolation threshold for the C–S–H phase has previously been predicted to be about 17–18% [23]. If, in the frozen paste, the conductivity of the C–S–H gel is much greater than the frozen pore solution, then the overall d.c. conductivity should appear to go to nearly zero near the true percolation threshold. Below this threshold, the C–S–H is disconnected, and the overall conductivity is dominated by the much smaller frozen pore fluid conductivity. In this case, the experimental threshold is in good agreement with the

*Two-point IS measurements tend to give somewhat higher low-frequency dielectric constants than do four-point measurements. The two-point measurements can give up to a three order of magnitude drop in k upon initial freezing, while the four-point measurements give closer to a two order of magnitude drop.

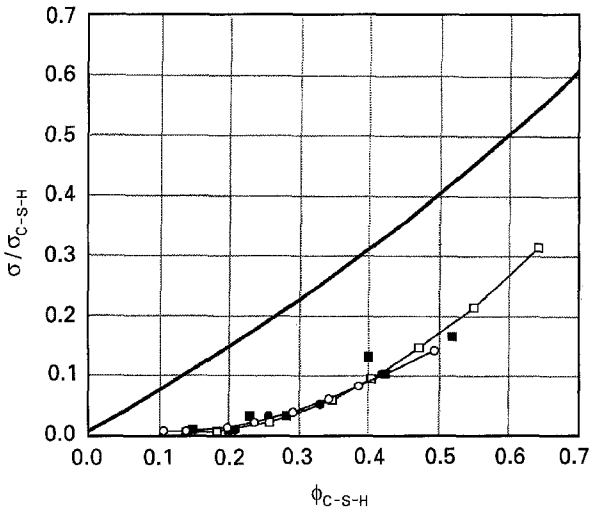

Figure 11 Normalized conductivity at − 40 °C versus the volume fraction of C–S–H for Portland cement pastes of w/c ratios (■) 0.4 and (●) 0.7. (□) NIST/NU (0.4), (○) NIST/NU(0.7), (——) H–S (0.4, 0.7).

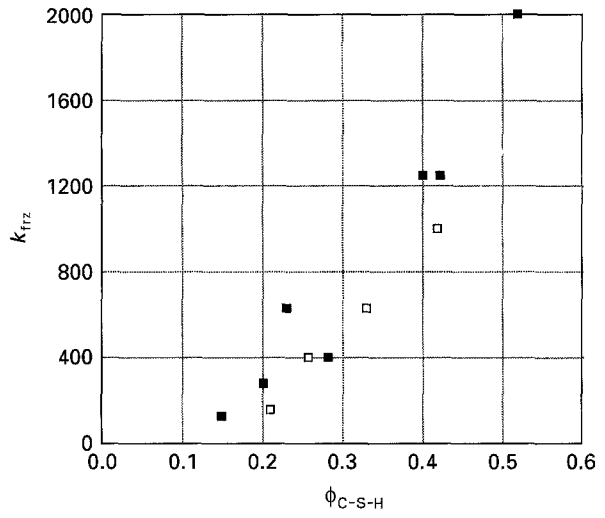

Figure 12 Relative dielectric constant at − 40 °C versus the volume fraction of C–S–H for Portland cement pastes of w/c ratios (■) 0.4 and (□) 0.7.

theoretical prediction. This threshold could also be the point at which the C–S–H network is physically strong enough to resist the stresses associated with freezing so that it is not broken apart and remains interconnected in the frozen cement paste. In this case, the true geometric percolation threshold for the C–S–H phase would be somewhat lower than the 17–18% theoretical prediction.

As shown by Fig. 12, the dielectric constant increases with the volume fraction of C–S–H gel for frozen pastes of w/c ratios 0.4 and 0.7, an indication that the C–S–H gel has the highest dielectric constant in the matrix. Moreover, the results for different w/c ratios are the same, further indicating that the dielectric behaviour of frozen cement paste depends only on its C–S–H content. This is another indication in support of the proposed dielectric amplification mechanism. In the frozen system, with the capillary pores "turned off", the values of σ/σ_{CSH} and possibly that of k follow a simple function of ϕ_{CSH}, without amplification of the value of k at the micrometre cement paste level. However, there is almost certainly still amplification at the C–S–H nanometre scale, as will be discussed further below.

It was found previously [25] that for the different cement paste phases, the percolation probabilities (a fraction of a given phase that is connected) for each phase at different w/c ratios all fell on the same curve when plotted against the volume fraction of that phase. The connectivity of each phase was independent of w/c ratio. Because the conductivity of a phase depends sensitively on how well it is connected, it was predicted [29] that the conductivity of unfrozen pastes would depend only on capillary porosity, the main conducting phase at room temperature, not the w/c ratio. Figs. 11 and 12 show that this is true also for the frozen pastes, when plotted against the volume fraction of C–S–H gel, the main conducting phase in the frozen state.

Fig. 11 also shows finite-difference computations from the NIST/NU cement paste microstructure model [29] for σ/σ_{C-S-H}, which are in excellent agreement with the experimental results. The C–S–H percolation threshold, and the arrangement of C–S–H compared to the arrangement of capillary pores are built right into this model, lending support for the above microstructural deductions from the electrical data. Effective medium theories like the general effective medium theory (GEM) [30] are not suitable for this material because there are three phases involved, two conducting and one insulating, and the GEM, at present, is set up for only two conducting phases. Fig. 11 also shows the Hashin/Shtrikman (H–S) exact upper bound for a three-phase material [31]. The corresponding H–S lower bound is identically zero. The H–S lower bound has a series-like microstructure built into it, so that the whole lower bound becomes zero if any one phase has zero conductivity [31]. In this case, we are assuming that the insulating phases actually have zero conductivities.

The actual values of the conductivity of each phase can be determined by a combination of experimental and model results. There are two parameters to be determined, expressed in the following way: (1) the ratio of the conductivity of pore fluid, σ_{pf}, to the conductivity of C–S–H, σ_{CSH}, at − 40 °C, and (2) the actual value of σ_{CSH} at − 40 °C. The value of the ratio needed to make the computations agree with experimental results was estimated by comparing the conductivity of frozen extracted pore solutions to the frozen cement paste. The frozen cement paste conductivities were much larger than that of the frozen pore solution. The value of σ_{CSH}/σ_{pf} was found to be about 100, which was then the value chosen to calculate the H–S bound and with which to run the digital-image-based microstructure model computation. Having this ratio is enough to compute the value of σ/σ_{CSH} in both cases, because normalizing the overall conductivity by σ_{CSH} reduces the number of parameters needed to only one. However, to extract the actual value of σ_{CSH} required the use of the experimental data, as follows.

The conductivity data at − 40 °C were preliminarily normalized by the conductivity of the sample with the longest hydration time, having therefore the

largest degree of hydration. This degree of hydration is known [4]. The model results were then also normalized by the model result at this same degree of hydration, and compared to the normalized experimental results. The agreement was extremely good, as good as in Fig. 11. The experimental value of σ/σ_{C-S-H} was then known accurately, from the model results, for each degree of hydration of the cement paste samples. Knowing σ experimentally for each sample then allowed σ_{C-S-H} to be determined for each sample at $-40\,^{\circ}C$. This calculated value did not vary more than 20% or so, over different degrees of hydration and the two different w/c ratios, 0.4 and 0.7, lending validity to this procedure. The value of σ_{C-S-H} at $-40\,^{\circ}C$ was found to be 6×10^{-5} Sm^{-1}, which was then used to normalize the experimental data at $-40\,^{\circ}C$.

In similar fashion, it should be possible to estimate the relative dielectric constant of C–S–H from the frozen paste data and the NIST/NU cement paste microstructure model. This work is in progress and will be reported separately. Nevertheless, the order of magnitude can be estimated based upon the data in Fig. 10. Concentrating at $-10\,^{\circ}C$, which ensures that all the gel porosity is unfrozen, the relative dielectric constant increases steadily with hydration time, from ~650 at 15 h to ~1250 at 26 h, ~2800 at 200 h, and finally ~4000 at 40 days, where C–S–H makes up approximately 50% of the microstructure by volume. These large values indicate that C–S–H gel is itself a microstructure that amplifies its dielectric constant. Gel pores and intervening C–S–H layers achieve amplification on the nanometre scale after the model in Fig. 3. The dielectric constant is amplified from 10 (solid phase) or 80 (pore fluid) to several thousand (C–S–H gel). Subsequently, above the melting point of the large capillary pores, the dielectric constant can be amplified further from $\sim10^3$ (C–S–H gel) to as high as 10^5 in pastes with a low degree of hydration. Here the large capillary pores and intervening C–S–H product layers achieve dielectric amplification on the micrometre scale, again after the model in Fig. 3.

6. Freeze-thaw cycling experiment

A possible application of being able to measure the dielectric properties of cement paste is demonstrated in Fig. 13, which shows the relative dielectric constant, measured at room temperature, of a white cement paste of w/c ratio 0.4, hydrated for 96 h, that was subjected to five freeze-thaw cycles. The lowest temperature reached in each cycle was decreased on each consecutive cycle. The room-temperature dielectric constant tended to drop after each cycle. This is possibly due to the expansive forces created by the freezing pore solution, which may have damaged the C–S–H phase, and thereby reduced the relative dielectric constant of the paste by changing the dielectric properties of the C–S–H phase. Note that in Fig. 13 the value of k drops below the nominal value for pure C–S–H, 10^3 [11], as the low-temperature end of the freezing cycle is decreased. After a few cycles, however, the dielectric constant of the frozen paste did not continue to decrease with cycling.

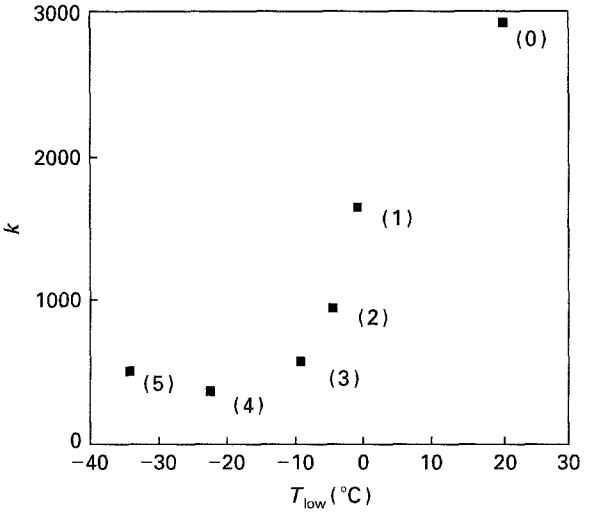

Figure 13 Relative dielectric constant versus end-point temperature for a 96 h 0.4 w/c white cement paste. The number of freeze–thaw cycles undergone is shown in parentheses for each data point. Each successive cycle reached a lower end-point temperature, which is the abscissa of the graph. Measurements were performed at room temperature when the sample reached equilibrium.

The results shown in Fig. 13 imply that dielectric constant measurements may be sensitive to changes in C–S–H microstructure, during freeze–thaw cycling and during other processes. This can only be true because of the sensitive dependence of the value of k on the microstructure, coming from the dielectric amplification mechanism that has been demonstrated in Part II of this series and further supported by the present work.

7. Conclusions

1. The dielectric amplification mechanism in cement paste comes from the microstructural relationship between the capillary porosity and the C–S–H gel phase. The large drop in the dielectric constant at the freezing point of the capillary pores indicates that the amplification occurs within the capillary pore network. The amplification may result from layers of C–S–H gel within the capillary pore network acting as small capacitors. Disconnected (not percolated) capillary pores are not required for the mechanism to be operative.

2. The magnitude of the large drop in both σ and k upon the first freezing of the larger capillary pores correlates well with the predicted percolation threshold of 18% for these pores [25], because when the cement paste samples reached a degree of hydration such that their capillary pore systems became disconnected, this large drop in properties vanished.

3. The influence of the C–S–H gel was found to dominate the electrical properties of the frozen cement paste matrix. The conductivity of frozen cement paste was successfully related to the volume fraction of C–S–H gel using the NIST/NU digital-based computer model.

4. Freezing the cement paste enabled the contributions of the capillary pores and the C–S–H phase to be approximately separated. Studying the frozen pastes,

where the C–S–H gel is the main conductor, showed that the percolation threshold for C–S–H is at a volume fraction of about 18%–20%, in good agreement with an earlier prediction [25].

5. The conductivity of the C–S–H phase, σ_{CSH}, at $-40\,^{\circ}C$, for both 0.4 and 0.7 w/c Portland cement pastes and for different degrees of hydration, was determined to be approximately $6 \times 10^{-5}\ S\ m^{-1}$, for lower than its value at room temperature.

Acknowledgements

Partial financial support for this work was provided by the National Science Foundation, through the Center for Advanced Cement-Based Materials. The authors also thank J. F. Douglas, NIST, for useful conversations and for providing important references.

References

1. B. J. CHRISTENSEN, T. O. MASON and H. M. JENNINGS, *J. Am. Ceram. Soc.* **75** (1992) 939.
2. B. J. CHRISTENSEN, R. T. COVERDALE, R. A. OLSON, S. J. FORD, E. J. GARBOCZI, T. O. MASON and H. M. JENNINGS, *ibid.* **77** (1994) 2789.
3. R. T. COVERDALE, E. J. GARBOCZI, H. M. JENNINGS, B. J. CHRISTENSEN and T. O. MASON, *ibid.* **76** (1993) 1513.
4. B. J. CHRISTENSEN, PhD Thesis, Northwestern University (1993).
5. C. A. SCUDERI, T. O. MASON and H. M. JENNINGS, *J. Mater. Sci.* **26** (1991) 349.
6. B. J. CHRISTENSEN, T. O. MASON and H. M. JENNINGS, *Mater. Res. Soc. Symp. Proc.* **245** (1991) 271.
7. P. GU, P. XIE, J. J. BEAUDOIN and R. BROUSSEAU, *Cem. Concr. Res.* **22** (1992) 833.
8. *idem. ibid.* **23** (1993) 157.
9. P. XIE, P. GU, Z. XU and J. J. BEAUDOIN, *ibid.* **23** (1993) 359.
10. R. T. COVERDALE, B. J. CHRISTENSEN, T. O. MASON, H. M. JENNINGS, E. J. GARBOCZI and D. P. BENTZ, *J. Mater. Sci.*, in press.
11. *idem, ibid.* **29** (1994) 4984.
12. J. R. MACDONALD (ed.), "Impedance Spectroscopy – Emphasizing Solid Materials and Systems", (Wiley, New York, 1987) p. 195.
13. P. N. SEN, *Geophysics* **46** (1981) 1714.
14. F. BROUERS, A. RAMSAMUGH and V. V. DIXIT, *J. Mater. Sci.* **22** (1987) 2759.
15. C. L. JACKSON and G. B. MCKENNA, *J. Chem. Phys.* **93** (1990) 9002.
16. B. A. BOUKAMP, "Equivalent Circuit (EQUIVCRT.PAS)", University of Twente; Department of Chemical Technology; P. O. Box 217-7500 AE Enschede; The Netherlands (1988).
17. R. DEFAY, I. PRIGOGINE, A. BELLEMANS and D. H. EVERETT, "Surface Tension and Adsorption" (Wiley, New York, 1966).
18. R. E. BEDDOE, and M. J. SETZER, Cem. Concr. Res. **18** (1988) 249.
19. C. DE FONTENAY and E. J. SELLEVOLD, in, "Durability of Building Materials and Components", ASTM STP 691, Edited by P. J. Serada and G. G. Litvan (American Society for Testing and Materials, Philadelphia, PA, 1980) p. 425.
20. F. H. WITTMANN, *J. Am. Ceram Soc.* **56** (1973) p. 409.
21. B. ZECH and M. J. SETZER, *Mater. and Struct.* **21** (1988) 323.
22. H. BAGER and E. J. SELLEVOLD, *Cem. Concr. Res.* **16** (1986) 709.
23. *Idem, ibid.* **16** (1986) 835.
24. N. BANTHIA, M. PIGEON and L. LACHANCE, *ibid.* **19** (1989) 939.
25. D. P. BENTZ and E. J. GARBOCZI, *ibid.* **21** (1991) 325.
26. S. S. YOON, S. Y. KIM and H. C. KIM, *J. Mater. Sci.* **29** (1994) 1910.
27. S. J. FORD, T. O. MASON, B. J. CHRISTENSEN, R. T. COVERDALE, H. M. JENNINGS and E. J. GARBOCZI, *J. Mater. Sci.* in press.
28. S. MINDESS and J. F. YOUNG, "Concrete" (Prentice-Hall Englewood Cliffs, NJ, 1981) p. 104.
29. E. J. GARBOCZI and D. P. BENTZ, *J. Mater. Sci.* **27** (1992) 2083.
30. D. S. MC LACHLAN, M. BLASZKIEWICZ and R. E. NEWNHAM, *J. Am. Ceram. Soc.* **73** (1990) 2187.
31. Z. HASHIN, *J. Appl. Mech.* **50** (1983) 481.

Received 22 December 1994
and accepted 2 May 1995